Z. Phys. C – Particles and Fields 46, 537–546 (1990)

Zeitschrift für Physik C Particles and Fields

Exclusive τ decays with the CELLO detector at PETRA

CELLO Collaboration

H.J. Behrend, L. Criegee, J.H. Field[1], G. Franke, H. Jung[2], J. Meyer, O. Podobrin, V. Schröder, G.G. Winter
Deutsches Elektronen-Synchrotron, DESY, Hamburg, Federal Republic of Germany

P.J. Bussey, A.J. Campbell, D. Hendry, S. Lumsdon, I.O. Skillicorn
University of Glasgow, Glasgow, UK

J. Ahme, V. Blobel, W. Brehm, M. Feindt, H. Fenner, J. Harjes, J. Köhne, J.H. Peters, H. Spitzer
II. Institut für Experimentalphysik, Universität, Hamburg, Federal Republic of Germany

W.D. Apel, J. Engler, G. Flügge[2], D.C. Fries, J. Fuster[3], P. Gabriel, K. Gamerdinger[4], P. Grosse-Wiesmann[5], M. Hahn, U. Hädinger, J. Hansmeyer, H. Küster[6], H. Müller, K.H. Ranitzsch, H. Schneider, R. Seufert
Kernforschungszentrum Karlsruhe und Universität, Karlsruhe, Germany

W. de Boer, G. Buschhorn, G. Grindhammer[7], B. Gunderson, C. Kiesling[8], R. Kotthaus, H. Kroha, D. Lüers, H. Oberlack, P. Schacht, S. Scholz, W. Wiedenmann[9]
Max-Planck-Institut für Physik und Astrophysik München, Federal Republic of Germany

M. Davier, J.F. Grivaz, J. Haissinski, V. Journé, D.W. Kim, F. Le Diberder, J.J. Veillet
Laboratoire de l'Accélérateur Linéaire, Orsay, France

K. Blohm, R. George, M. Goldberg, O. Hamon, F. Kapusta, L. Poggioli, M. Rivoal
Laboratoire de Physique Nucléaire et Hautes Energies, Université de Paris, Paris, France

G. d'Agostini, F. Ferrarotto, M. Iacovacci, G. Shooshtari, B. Stella
University of Rome and INFN, Rome, Italy

G. Cozzika, Y. Ducros
Centre d'Études Nucléaires, Saclay, France

G. Alexander, A. Beck, G. Bella, J. Grunhaus, A. Klatchko, A. Levy, C. Milstène
Tel Aviv University, Tel Aviv, Israel

Received 2 January 1990

Abstract. We present high precision results from an analysis of all major τ branching ratios, determined simultaneously in the same experiment. The results are based on 6064 τ decays observed at $\sqrt{s}=35$ GeV, using the CELLO detector at PETRA. The sum of the measured exclusive branching ratios saturates the total τ decay width. In a comparison with the topological branching ratios measured recently by CELLO, the sums of the respective exclusive branching ratios are found to saturate the inclusive fractions. Our results are in good general agreement with existing measurements. However, the decay fractions for $\tau^- \to \pi^- \pi^+ \pi^- \nu_\tau$ and $\pi^- \to \pi^- \pi^0 \pi^0 \nu_\tau$ are larger than the present world averages. All measured branching ratios are in good agreement with the expectations from a standard τ lepton.

[1] Now at Université de Genève, Switzerland
[2] Now at RWTH, Aachen, FRG
[3] Now at Instituto de Fisica Corpuscular, Universidad de Valencia, Spain
[4] Now at MPI München
[5] Now at SLAC, Stanford, USA
[6] Now at DESY
[7] On leave of absence at SLAC
[8] Heisenberg-Stipendiat der Deutschen Forschungsgemeinschaft
[9] Now at CERN

1 Introduction

Since the discovery of the τ lepton by Perl et al. [1] in 1975, its production and decay properties have been

subject to intensive investigations. In the framework of the standard theory of electroweak interactions [2] the τ lepton and its associated neutrino ν_τ are placed in a third ("sequential") lepton doublet in addition to the electron and the muon doublets. With this assignment, the τ is produced in pairs in e^+e^- annihilations via photon and Z^0 boson exchange. The weak τ decays to purely leptonic and semihadronic final states are mediated by the $W^\pm$ bosons coupling to the weak charged lepton and quark currents. The mass of the τ allows coupling only to the first quark doublet, consisting of the u and the Cabibbo-rotated d_C quark fields.

τ production in e^+e^- interactions has been well studied and the experimental results concerning the cross section and charge asymmetry are in good agreement with standard theoretical expectations (see, e.g., [3] for a recent compilation). The decays, on the other hand, have so far not been completely understood. A major part of the decay modes can be calculated reliably [4–6] and these decays have indeed been observed with the expected branching ratios (see [7–9] for recent reviews). However, the sum of existing measurements of the individual branching fractions combined with theoretical constraints on unmeasured channels leaves room for about 5% of so far unobserved decay modes [10]. Within the framework of the standard model, there seems to be little hope to explain the discrepancy with expected but so far unmeasured decay channels [11]. A comparison with measurements of the topological branching ratios (denoted by BR_1, BR_3, BR_5 for decays into one, three or five charged particles plus neutrals) shows that the "missing" decay channels have to be attributed to the one-prong decays. The comparison relies on data to be combined from many different experiments. To minimize the role of experimental bias or inadequately estimated systematics [8], for a better understanding of τ decays it is very desirable to determine both the inclusive and exclusive decay modes in the same experiment.

In a high statistics experiment using the CELLO detector at PETRA we have measured the topological and all the major exclusive τ decay fractions simultaneously. Our results for BR_1, BR_3 and BR_5 have been published previously [12]. Here we give measurements of branching fractions of the major exclusive τ decay modes, including the previously poorly determined multiple π^0 decays [13]. Our measurements present a consistent picture of the τ decay pattern in good agreement with conventional expectations.

2 Experiment

2.1 Detector

The data presented here come from a high statistics experiment at 35 GeV c.m. energy, in which $87 pb^{-1}$ were collected with the CELLO detector. CELLO is a general purpose magnetic detector, equipped with a fine grain lead liquid argon electromagnetic calorimeter. Charged particles are measured over 91% of the full solid angle in a cylindrical detector made of interleaved drift and proportional chambers inside a $1.3\,T$ magnetic field, yielding a momentum resolution of $\sigma(p)/p = 0.02\,p$ (p in GeV/c) without and $0.01\,p$ with vertex constraint. Electrons and photons are detected and identified in the barrel part of the calorimeter (20 radiation lengths thick at normal incidence) which covers a solid angle of 86% of 4π. The calorimeter has both good energy ($\sigma(E)/E = 0.05 + 0.1/\sqrt{E}$ (E in GeV)) and angular (6 to 10 mrad) resolution which is important for the reconstruction of π^0's especially in final states with high photon multiplicities. Muons are detected outside the 80 cm thick iron return yoke by large planar drift chambers covering 92% of 4π. The experiment was triggered by various combinations of charged particle and calorimeter triggers, making use of a fast track finding hardware [14] and of the time structure of the liquid argon signal to suppress background. Further details on the detector can be found elsewhere [15].

2.2 Particle identification

One of the crucial properties of the detector in detecting all τ decay channels is its ability to identify electrons, muons, hadrons and photons. Electrons are identified by their characteristic shower pattern in the calorimeter, with the total deposited energy matching the momentum measured in the central detector. Muons are identified by a hit in the muon chambers and a shower pattern compatible with a minimum ionising particle. All other charged particles are considered as hadrons (discrimination of charged pions from kaons is not possible with CELLO). Photons are detected as electromagnetic showers in the calorimeter without associated track in the central detector. π^0's were found either by a fit of two photons to the π^0-mass (with a probability cut $P(\chi^2) > 0.01$) or by a single broad shower compatible with overlapping photons. The distribution of the χ^2 probabilities for the fits to a π^0 hypothesis from all photon-photon combinations in the multiphoton final states is shown in Fig. 1. Only combinations with $P(\chi^2) > 0.01$ were accepted (see above). The flatness of this distribution shows that the energy and angular errors of the photons reconstructed from the calorimeter information are reasonable well understood.

To determine accurately the various probabilities for particle identification and misidentification, extensive Monte Carlo simulations of the particle response in the experiment have been carried out. The shower Monte Carlo simulation is done by EGS [16] for electromagnetic particles and by HETC [17] for hadrons. The predicted probabilities for charged particles, which play an important role in the measurement of the exclusive branching ratios, were compared with experimental determinations on reference samples taken from radiative Bhabha events (electrons), from cosmic rays (muons), and from the reaction $\gamma\gamma \to \rho^0\rho^0$ and from three-prong τ decays (charged hadrons). The comparison was done for various momentum ranges. The results averaged over all momenta are shown in Table 1. To investigate sys-

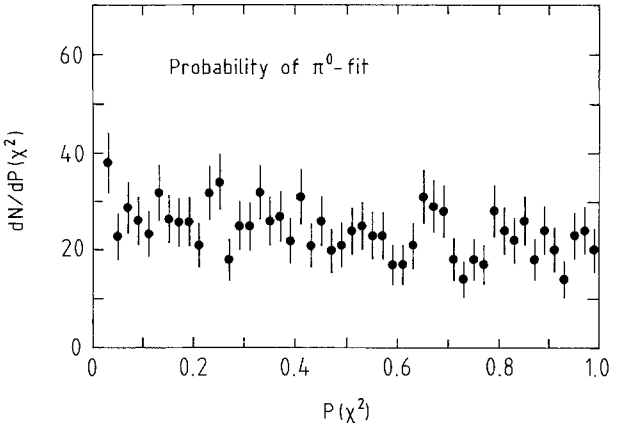

Fig. 1. Distribution of the χ^2 probabilities for the fits to a π^0 hypothesis from all photon-photon combinations in the multiphoton final states. Only the combinations with $P(\chi^2)>0.01$ are shown

tematic effects, we varied the identification criteria within reasonable limits. Good agreement between the results for data and Monte Carlo is observed for all momenta and all identification criteria. The systematic error due to charged particle identification is limited by the reference data statistics ($\sim$9000 events for each particle type) and is below 1%.

To demonstrate our ability to reconstruct π^0's from identified photons we show in Fig. 2 a comparison of two photon invariant mass spectra for simulated and real τ decays into one charged particle and an arbitrary number of photons (for the τ event selection see Sect. 3 and [12]). A clear π^0 signal and good agreement between experimental data and Monte Carlo predictions is observed for all photon multiplicities. The predicted photon detection efficiency is about 60% for $E_\gamma<1$ GeV and about 80% for $E_\gamma>1$ GeV in events of this type.

Fig. 3a shows the invariant mass distribution of final states consisting of one charged particle and two photons, where the photons fit well ($P(\chi^2)>0.01$) to the π^0-mass. Such final states are expected to be dominated by the decay $\tau\to\rho\nu$, $\rho\to\pi\pi^0$. We observe a clean ρ-signal both in data and Monte Carlo. As a further example of the combination of calorimetric and tracking information and its proper reproduction by the Monte Carlo, we show in Fig. 3b the invariant mass distributions of final states from τ decays leading to one charged particle and one observed neutral shower without further requirements. These final states are also expected to be dominated by the decay $\tau\to\rho\nu$, $\rho\to\pi\pi^0$, where the π^0 either has a large momentum so that the two decay photons are not separated, or decays asymmetrically with a low energy photon undetected. The ρ mass peak is well reproduced as is the accumulation at low masses which originates from background due to radiative electrons and misidentified photons close to a charged hadron (most likely fragments of the hadronic shower). Requiring the charged particle to be a hadron and eliminating photons forming an opening angle less than 3° with the charged particle leads to a ρ signal almost free of background (Fig. 3c). The small mass shift in this distribution is due to the unobserved photon.

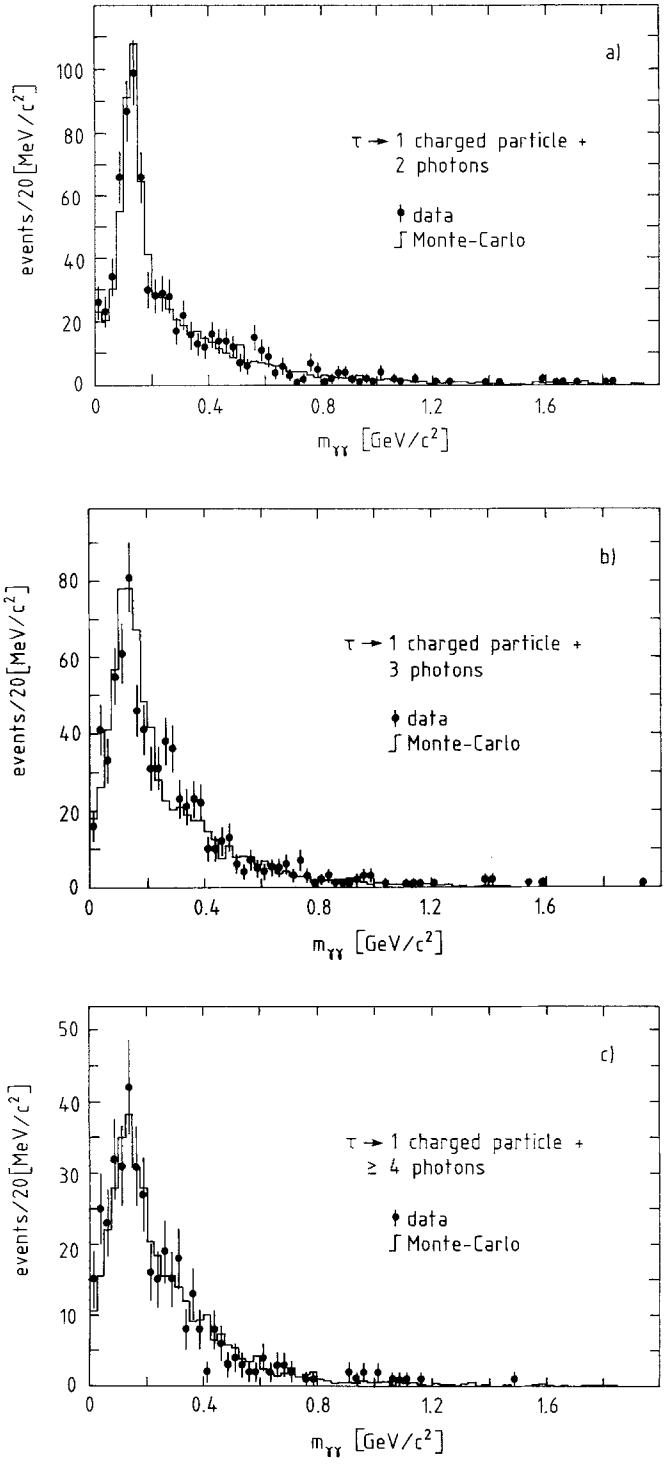

Fig. 2a–c. Invariant mass of two photons in τ decays with one charged particle and **a** two observed photons, **b** three observed photons, **c** four or more observed photons. The data points and the Monte Carlo predictions (histograms) are shown

Systematic errors due to photon detection efficiency were investigated by varying the photon identification cuts over a wide range. The ρ-signal is not sensitive to this variation and we conclude that the contribution to the systematic error in the exclusive branching ratios, originating from photon identification, is below 1%.

Table 1. The particle identification matrix $\eta_{i\to j}$ $(i, j = e, \mu, h)$ for data and Monte Carlo averaged over all momenta. $\eta_{i\to j}$ is the probability (in %) that a particle of type i is identified as particle of type j. Quoted errors are purely statistical. The tracking efficiency is not included

$i\to$	3		μ		h	
$j\downarrow$	MC	Data	MC	Data	MC	Data
e	88.8±0.3	88.7±0.5	1.0±0.1	1.0±0.2	2.5±0.1	2.7±0.2
μ	0.5±0.1	0.4‡	77.3±0.3	77.6±0.4	4.0±0.1	4.5±0.2
h	10.7±0.3	11.0±0.5	21.7±0.3	21.3±0.4	93.5±0.2	92.8±0.3

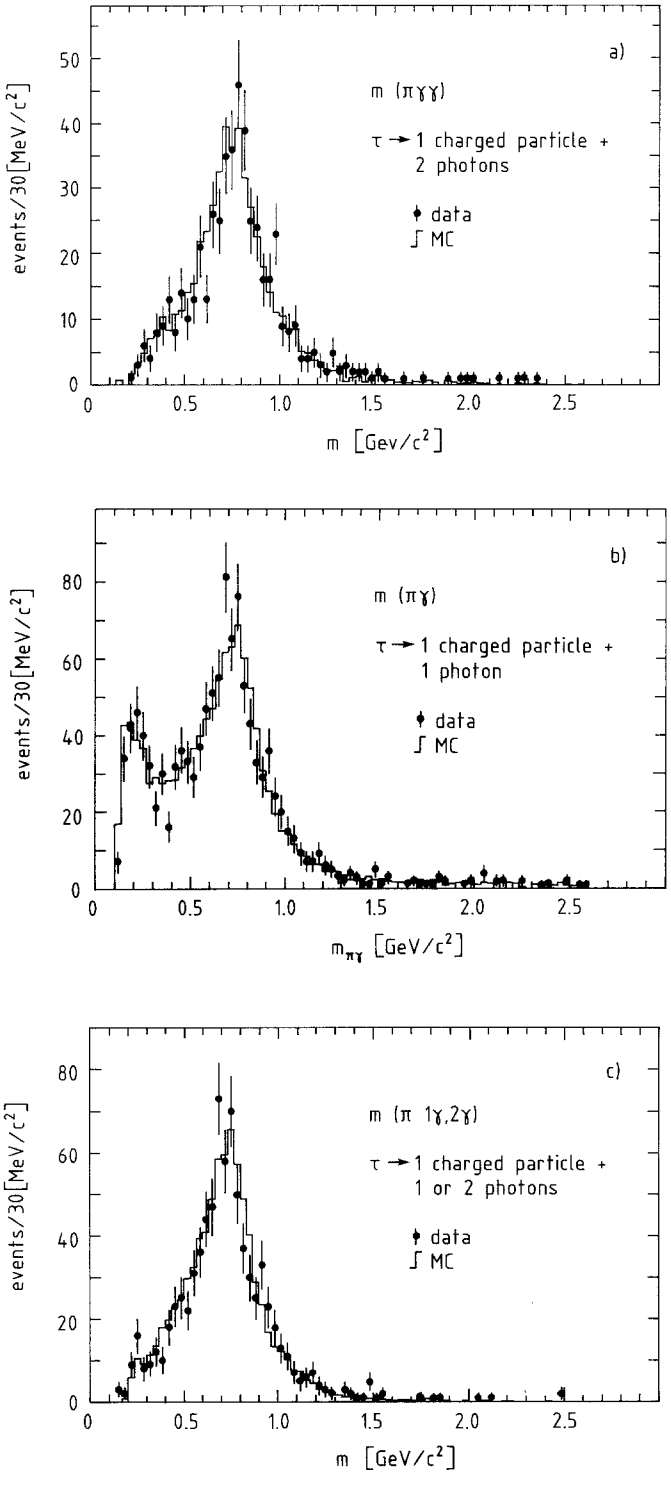

3 Event selection and background estimation

τ pair candidates are selected with a series of cuts taking advantage of the special topology and kinematics of the τ pair final state. Only the most important cuts will be given here, further details of the selection procedure have been published previously [12, 18]. Using all charged and neutral particles in an event the sphericity axis is determined and divides the event in two hemispheres. The particles in each hemisphere in turn are used to construct individual "jet" axes. The angles used below are defined with respect to these two jet axes. A cut in the acollinearity angle ($0.5° < \alpha_{\text{acol}} < 50°$) removes a large part of Bhabha, μ pair, cosmic ray, two photon and radiative τ pair events. The remaining background from two photon collisions and Bhabha events is removed by rejecting events with two identified electrons or muons, and by a cut in the acoplanarity angle ($0° < \alpha_{\text{acop}} < 40°$) and the total energy in the central barrel calorimeter ($0.05\sqrt{s} < E < 0.75\sqrt{s}$). Multihadronic events are almost completely eliminated by restricting the maximum number of charged particles to 10 and limiting the invariant mass of all charged and neutral particles in each hemisphere of a candidate event to less than 2.7 GeV/c^2. Finally, cosmic ray events are efficiently removed by demanding a minimum opening angle of 0.5° in the Rz-projection between the tracks in the wire chamber. To retain as many τ decays as possible loose selection cuts were first chosen, and the selected events (4756) were subjected to a visual scan. After this scan, 3032 events survived. As can be seen from Table 2, the bulk of the rejected events were QED events (with electrons or photons pointing to cracks between the calorimeter segments), or multihadronic and two-photon induced events with unreconstructed tracks at small angles with the colliding beams. Furthermore 29 beam-gas events and 190 cosmics were identified, which are not contained in the table. To check the scanning procedure, a Monte Carlo sample of equivalent statistical signifi-

Fig. 3a–c. Invariant mass distribution of: **a** one charged particle and two photons forming a π^0, **b** one charged particle and one photon without further requirements, **c** one charged particle and one photon, where identified electrons and low energy photons close to the charged particle (most likely fragments of the hadronic shower) are removed. The data points and the Monte Carlo predictions (histograms) are shown

Table 2. Numbers of events classified by visual scan for 4 sets of increasingly tighter selection cuts (e.g. variation of the maximal energy in the calorimeter from $0.75\sqrt{s}$ in 4 roughly equidistant steps down to $0.50\sqrt{s}$, see also [12]). The final analysis is based on cut set 1. The classification is: good τ pairs ($\tau\tau$), possible τ pairs ($\tau\tau$(?)), QED events ($ee(\gamma\ldots)$, $\mu\mu(\gamma)$), multihadronic events ($q\bar{q}$), two-photon induced events ($\gamma\gamma$) and unclear events(?). The Monte Carlo events for the various physics channels are calculated using the known cross section at $\sqrt{s}$ = 35 GeV and with the same integrated luminosity as the data. The Monte Carlo numbers are thus absolute predictions

Reaction	Cut set 1		Cut set 2		Cut set 3		Cut set 4	
	MC	Data	MC	Data	MC	Data	MC	Data
$\tau\tau$	3077	3032	2665	2636	2337	2272	2073	2017
$\tau\tau$(?)	52	50	35	40	29	35	11	33
$ee(\gamma\ldots)$	1000	991	477	433	275	225	151	145
$\mu\mu(\gamma)$	70	60	52	32	42	17	37	13
$q\bar{q}$	112	97	71	81	54	68	48	62
$\gamma\gamma$	267	254	214	194	171	156	160	142
?	51	53	33	40	27	34	20	31

cance to the data, containing both τ pair events and background, was generated using a full simulation of the detector, was processed through the same reconstruction and selection programs as the data and was subsequently scanned.

The remaining background in the sample of 3032 τ pair candidates has been determined by Monte Carlo and amounts to a total of 7%, dominated by radiative Bhabha events (2.5%) and the two-photon channels $e^+e^- \to e^+e^-\mu^+\mu^-$, $e^+e^-\tau^+\tau^-$ (3.5%). The background from residual multihadronic events (0.5%) was determined from Monte Carlo events $e^+e^- \to$ hadrons. By comparison with multihadronic events from the same experiment, restricting one of the two jets to τ-like topologies ($\leqq$3 charged particles, invariant mass $\leqq$3 GeV/c^2), it was verified that the Monte Carlo invariant mass distributions are correct. In addition, we estimated from our experimental multihadron data an upper limit (90% C.L.) of 30 multihadronic background events in the multiprong τ sample, which corresponds to 1% and is consistent with the Monte Carlo prediction.

To demonstrate the overall small background, distributions of the invariant masses for one-prongs (with at least one additional photon) and three-prongs (with any number of photons) in the τ pair events are shown in Fig. 4 for the data and the τ Monte Carlo. The invariant masses are calculated from the charged particles and the photons in each hemisphere separately. The τ Monte Carlo describes the observed distributions well.

The systematical uncertanties of the selection procedure were studied by varying the selection criteria. The cuts for the minimal acoplanarity angle and the maximal calorimeter energy were tightened in 4 steps (see [12] for further details). The result of this study is shown in Table 2, where the numbers of τ pair candidates and the various backgrounds are given for the 4 sets of selection cuts. In all cases good agreement is found between data and predictions, thus verifying both the Monte Carlo simulations and the scanning procedure in detail.

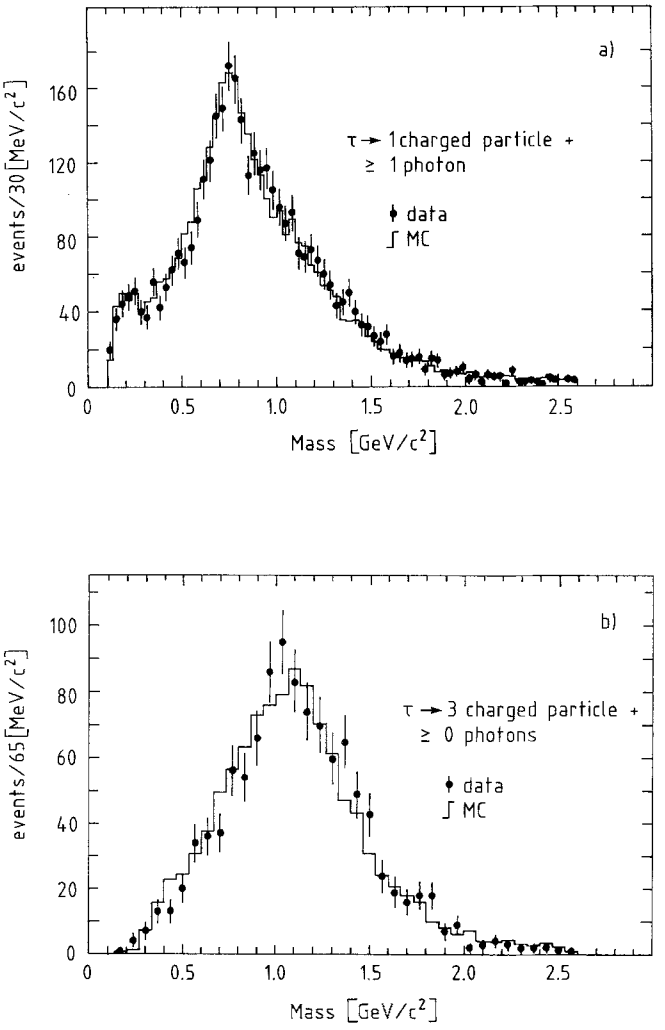

Fig. 4a, b. Invariant mass of the visible particles in τ decay. Charged particles and photons are used. The data points and the Monte Carlo predictions (histograms) are shown. **a** Invariant mass of one-prong decays with at least one additional photon, **b** invariant mass of three-prong decays with any number of photons

4 Analysis and results

4.1 Major exclusive τ decay modes

The branching ratios for the individual decay channels were determined in the following steps:

1. Classification of the τ decays into seven classes which largely correspond to the exclusive decay channels
2. Determination of a set of probabilities P_i for each τ-candidate to belong to one of the seven classes
3. Determination of the branching ratio of each class independently
4. Determination of the branching ratios of all classes simultaneously
5. Investigation of systematic uncertainties.

The τ decays are classified according to the main decay channels predicted by the standard model (see Table 3). The first two classes are the two leptonic decay modes, classes 3, 4 and 5 include all semihadronic decay modes with one charged particle and respectively zero, two, and more than two photons in the final state; class 6 is the three-prong decay mode without additional photons and class 7 includes all other multiprong decay modes. The classification is complete in the sense that all τ decays expected from the standard model can be assigned to one of the classes.

For each observed τ decay a set of probabilities $P_i(i=1, 2, \ldots, 7)$ has been determined, giving the probabilities to assign the decay to one of the classes i, using particle identification, the number of charged and neutral particles, and kinematic quantities such as particle momenta and invariant masses. As examples for such distributions used, we show in Fig. 5 the measured charged particle momentum spectra and the respective Monte Carlo predictions for the first four classes. Details on the method can be found elsewhere [19].

The probabilities P_i have been used in two ways to identify the τ decay channels, i.e. to attribute a given τ candidate to a specific class i:

1. The largest of the P_i was used to assign the decay to class i, thus forcing each τ decay into one of the seven classes.
2. Thresholds P_i^{cut} were introduced for each class and the largest element P_i had to satisfy the condition $P_i > P_i^{\text{cut}}$ in order to assign the decay to class i. With this method a certain number of τ candidates, depending on the value chosen for P_i^{cut}, were discarded.

The general idea of the analysis is to determine the branching ratios of the τ decay channels with method 1 and to verify with method 2 that we observed them all. For decays not contained in the seven classes above we expect low P_i values for all classes. A potentially incomplete model for the τ decay (e.g. the standard model we have chosen) could therefore be identified: As the threshold values P_i^{cut} in method 2 are increased, the number of discarded τ's in the data would become larger than expected from the underlying Monte Carlo model and the resulting exclusive branching ratios would no longer sum up to 100%.

The branching ratios BR_i are defined as N_i/N_{tot} where the true numbers N_i of τ decays in class i (for the full solid angle) are related to the observed numbers n_i by a transition matrix $\varepsilon_{i\leftarrow j}$, according to the relation

$$n_i - n_i^B = \sum \varepsilon_{i\leftarrow j} N_j. \tag{1}$$

n_i^B is the number of non-τ background events in class i and the matrix elements $\varepsilon_{i\leftarrow j}$ give the probability that class j is identified as class i, i.e. the diagonal elements $\varepsilon_{i\leftarrow i}$ are the efficiencies to detect class i. The total number of τ decays N_{tot} was taken from the analysis of the topological branching ratios [12] and is therefore indepen-

Table 3. Assignment of observed τ decays to the seven classes (see text). n_i/n_i^B denote the numbers of selected τ decays/non-τ background events for class i. Numbers are given separately for the two methods of assignment: a) "max P_i": the decay is assigned to the class of maximum probability b) "$P_i > P_i^{\text{cut}}$": the maximum probability also has to exceed the threshold P_i^{cut}. For the latter method a "garbage" class (no decay channel assigned) is filled. c) same as b) but with the hard selection cut set 4 (see Table 2). The branching ratios for each class using the above methods are also given with their statistical errors

Decay mode	Class	a) (cut set 1)		b) (cut set 1)		c) (cut set 4)	
		n_i/n_i^B max P_i	BR_i[%] max P_i	n_i/n_i^B $P > P_i^{\text{cut}}$	BR_i[%] $P > P_i^{\text{cut}}$	$P > P_i^{\text{cut}}$	$P > P_i^{\text{cut}}$
$\tau \to e\nu\nu$	1	684/ 40	18.6 ± 0.9	659/ 37	18.4 ± 1.0	447/11	18.3 ± 1.0
$\tau \to \mu\nu\nu$	2	606/ 38	17.9 ± 0.9	534/ 35	17.8 ± 1.0	339/ 4	17.5 ± 1.0
$\tau \to h\nu$	3	1531/193	12.6 ± 1.2	653/ 82	12.0 ± 1.4	396/ 9	12.0 ± 1.5
$\tau \to h + 2\gamma\nu$	4	1185/ 84	22.8 ± 1.6	917/ 77	23.0 ± 1.8	641/ 9	24.1 ± 1.9
$\tau \to h + > 2\gamma\nu$	5	967/ 29	14.2 ± 1.3	828/ 13	14.3 ± 1.4	575/ 3	13.7 ± 1.5
$\tau \to 3h\nu$	6	714/ 20	9.4 ± 1.2	550/ 10	8.4 ± 1.3	352/ 4	9.0 ± 1.3
$\tau \to 3(5)h + \geqq 1(0)\gamma\nu$	7	377/ 25	5.9 ± 1.2	153/ 15	6.3 ± 1.7	109/ 4	6.3 ± 1.9
rest				1770/159		1175/26	
Sum		6064/429	101.4 ± 3.2	4294/269	100.2 ± 3.6	4043/70	101.0 ± 3.9

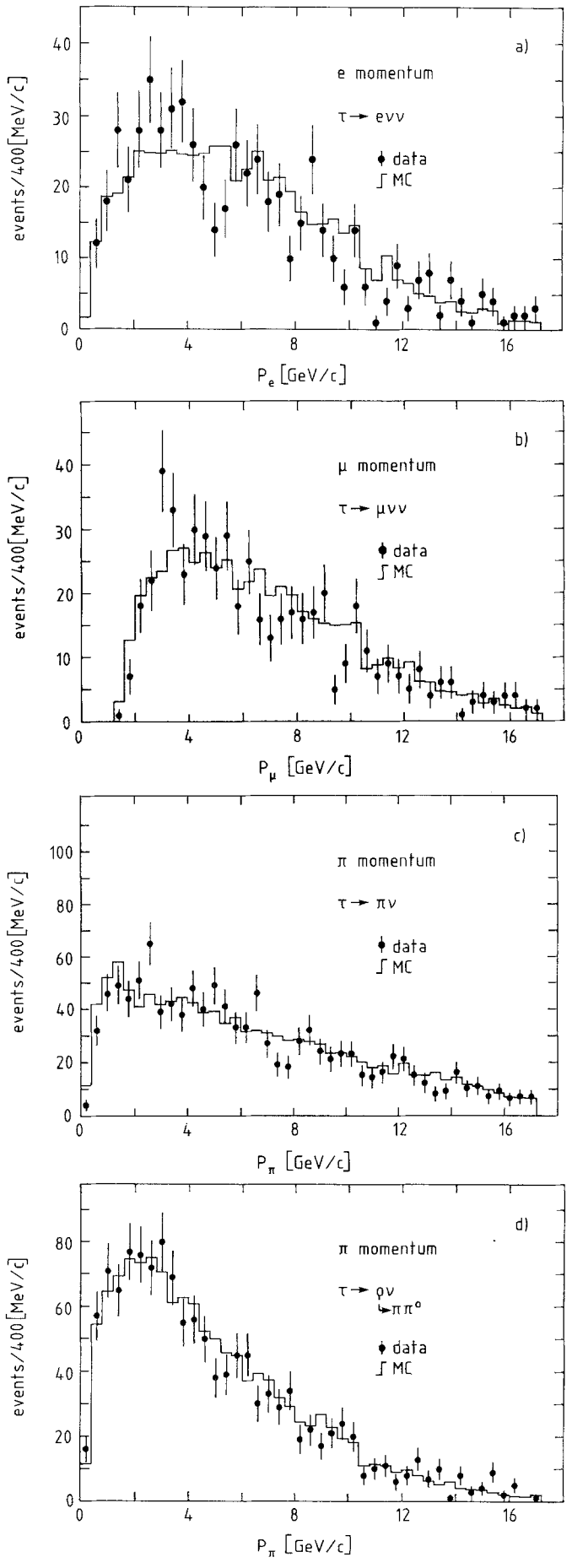

dent of this analysis. For both methods we have determined the matrix elements $\varepsilon_{i\leftarrow j}$ and the numbers of background events n_i^B, using the full Monte Carlo with input branching ratios taken from our measurements after iteration.

In a first step the branching ratios were determined for each class separately using the following relation

$$n_i - n_i^B = \varepsilon_{i\leftarrow i} N_i + \varepsilon_{i\leftarrow r}(N_{\text{tot}} - N_i) \tag{2}$$

as a special case of (1), where $\varepsilon_{i\leftarrow r}$ is the total probability to find a τ decay from any other class in class i. Table 3 shows the number n_i and n_i^B of events contained in each class for method 1, and for method 2 using the tightest threshold values P_i^{cut}. The distributions of the weights P_i depend on the decay channel considered and so do the thresholds P_i^{cut}: They were chosen between 0.2 and 0.55 for the classes containing one charged hadron and an arbitrary number of photons, and between 0.5 and 0.95 for the other classes [19]. For both methods the event sample has been selected according to the standard cut set 1. In addition, we show the numbers of observed decays in the various classes for method 2, using the tight selection cut set 4 (see also Table 2). For each method the resulting branching ratios are also listed. Within the statistical errors the results for the individual classes for all three determinations are in good agreement. Furthermore, the sum of the branching ratios calculated with method 2, treating each decay channel independently, saturates to 100% within the errors, suggesting that the τ decay classes considered in this analysis are complete.

With the completeness of the decay channels thus established, a likelihood method fitting all channels simultaneously was performed. Assuming Poisson statistics for the observed number of events n_i the following expression was minimised:

$$\mathscr{L} = \sum_i \{\sum_j \varepsilon_{i\leftarrow j} N_{\text{tot}} \,\text{BR}_i - (n_i - n_i^B)\ln(\sum_j \varepsilon_{i\leftarrow j}\,\text{BR}_j)\}. \tag{3}$$

As above, the branching ratios BR_i are defined as the ratios N_i/N_{tot}, where the N_i are the corrected numbers of τ decays in class i (see (1)). The full transition matrix $\varepsilon_{i\leftarrow j}$ of relation (1) used in the fit is shown in Table 4. The simultaneous fit of all τ decays has the advantage that the results, as we checked, are independent of the input branching ratios used in the Monte Carlo simulation and that the errors are minimized. The likelihood fit was done for both methods 1 and 2 of classifying the observed τ decays. The results obtained with method 2 for different thresholds P_i^{cut} always agreed with those of method 1. Table 5 shows the resulting branching ratios for the seven classes, together with their statistical and systematic errors.

Fig. 5a–d. Measured (points) and simulated (histogram) momentum distributions of final state charged particles in one-prong τ decays (classes 1 to 4 of Table 3): **a** Electrons assumed to come from $\tau \to e\bar{\nu}\nu$, **b** muons assumed to come from $\tau \to \mu\bar{\nu}\nu$, **c** hadrons assumed to come from $\tau \to \pi(K)\nu$, **d** pions assumed to come from $\tau \to \rho\nu$

Table 4. Transition matrix $\varepsilon_{i\leftarrow j}$, giving the efficiencies for assigning a τ decay in class j to class i. The matrix elements are given in % and include the acceptance correction. The quoted errors are due to the Monte Carlo statistics

	1	2	3	4	5	6	7
1	20.45±0.22	0.38±0.01	5.76±0.06	1.13±0.01	0.38±0.01	0.11±0.01	0.05±0.01
2	0.16±0.01	18.55±0.19	7.55±0.08	1.12±0.01	0.41±0.01	0.09±0.01	0.06±0.01
3	0.49±0.06	0.53±0.08	29.33±0.35	2.92±0.03	0.85±0.01	0.12±0.01	0.11±0.01
4	0.35±0.01	0.25±0.01	7.57±0.01	19.76±0.16	9.13±0.07	0.85±0.01	0.49±0.01
5	0.28±0.01	0.11±0.01	3.16±0.04	10.27±0.11	23.13±0.25	0.87±0.01	1.62±0.02
6	0.00±0.01	0.00±0.01	0.07±0.01	0.07±0.01	0.08±0.01	32.18±0.42	6.23±0.08
7	0.00±0.01	0.00±0.01	0.03±0.01	0.08±0.01	0.31±0.04	18.12±0.27	21.91±0.31

Table 5. Measurements of the exclusive branching ratios in % for the seven classes using the likelihood method (see text). The individual branching ratios within the classes 3, 4, 5 and 6 have been determined by subtracting the expected strange particle contributions. The errors quoted are statistical and systematic. The branching ratios for the seven classes are added up to yield the sum for this experiment. For comparison, the world averages from a recent compilation [20] are also given. The theoretical expectations are based on the standard model and are normalised using measurements of the τ lifetime (see, e.g., [7])

Decay channel	Class	this experiment	world av.	theor. expect.
$\tau \to e\nu\nu$	1	18.4 ±0.8±0.4	17.5±0.4	18.9±0.5
$\tau \to \mu\nu\nu$	2	17.7 ±0.8±0.4	17.8 ±0.4	18.4
$\tau \to$ hadron ν	3	12.3 ±0.9±0.5		
$\tau \to \pi\nu$		11.1 ±0.9±0.5	10.8 ±0.6	11.4
$\tau \to K\nu$			0.7 ±0.2	0.74
$\tau \to$ hadron $+2\gamma\nu$	4	22.6 ±1.5±0.7		
$\tau \to \rho\nu$		22.2 ±1.5±0.7	22.3 ±1.1	23.2
$\tau \to K\pi\nu$			1.4 ±0.3	1.2
$\tau \to$ hadron $+ > 2\gamma\nu$	5	14.0 ±1.2±0.6		
$\tau \to \pi 2\pi^0\nu$		10.0 ±1.5±1.1	7.5 ±0.9	9.0
$\tau \to \pi \geqq 3\pi^0\nu$		3.2 ±1.0±1.0	3.0±2.7	1.2
$\tau \to 3$ hadrons ν	6	9.0 ±0.7±0.3		
$\tau \to 3\pi\nu$		8.7 ±0.7±0.3	6.8 ±0.6	9.0
$\tau \to 3(5)$ hadrons $+ \geqq 1(0)\gamma\nu$	7	5.8 ±0.7±0.2		
$\tau \to 3\pi \geqq 1\pi^0\nu$		5.6 ±0.7±0.3	4.4 ±1.6	5.0
$\tau \to 5\pi \geqq 0\pi^0\nu$		0.16±0.14	0.12±0.03	
$\tau \to K\pi\pi\nu$			0.22±0.14	0.2
$\tau \to K\bar{K}\nu$				0.6
$\tau \to K\bar{K}\pi\nu$			0.22±0.15	0.2
$\tau \to 5\pi\nu$			0.06±0.02	0.2
$\tau \to 6\pi\nu$			0.05±0.02	0.2
Sum		99.8 ±2.6±1.2	92.8 ±3.6	100.0

Varying all independent input parameters ($\varepsilon_{i\leftarrow j}$, n_i^B and N_{tot}) within their uncertainties and refitting the branching ratios, we get a spread of results which determines their systematic errors. The systematic errors on the transition matrix elements receive contributions from uncertainties of the following quantities and procedures:

- selection, trigger and scan efficiencies
- particle identification
- photon detection efficiency
- τ decay identification (estimated by comparing different methods to determine the P_i)
- choice of threshold values P_i^{cut} (estimated by variation)
- unknown input branching ratios in the Monte Carlo simulation (estimated by variation).

Comparing the input and output branching ratios of a Monte Carlo test sample, we verified that the whole analysis chain is free of bias. Since in all comparisons of the Monte Carlo predictions with the data we observe agreement within statistics, the systematic errors on the n_i^B are conservatively assumed to be equal to the statistical one. Varying the different cuts involved in the selection of the τ final states over a wide range as described above, we observe consistent results for the branching ratios, well within the statistical uncertainties (see also Table 3).

With the known branching ratios for the τ into strange particles, the Cabibbo-allowed decays of the τ can be extracted from the classes 3 and 4 (see Table 5). Using the present world averages [20] BR($\tau \to K\nu$)

$=(0.7\pm0.2)\%$ and $BR(\tau\to K^*\nu)=(1.4\pm0.3)\%$ their contributions can be subtracted to yield the exclusive branching ratios for $\tau\to\pi\nu$ and $\tau\to\rho\nu$. Similarly, the K^* contribution was subtracted in class 6 to obtain the branching ratios for $\tau\to3\pi\nu$. To obtain the branching ratio for $\tau\to3\pi\geqq1\pi^0\nu$ we subtracted from the branching ratio for class 7 the contribution due to $\tau\to5\pi(\geqq0)\,\pi^0\nu$ which was determined to be $(0.16\pm0.14)\%$ in [12]. The systematic errors for the branching ratios of the Cabbibo-allowed decays entered in Table 5 contain the uncertainties on the various subtractions.

4.2 *Multi-π^0 τ decay modes*

In a further step the branching ratios of the decay modes $\tau\to\pi2\pi^0\nu$ and $\tau\to\pi\geqq3\pi^0\nu$ were determined. As already demonstrated in Fig. 1 the CELLO calorimeter allows us to reconstruct π^0's even in final states with high photon multiplicity. For each decay candidate with two or more observed photons we determined the number of π^0 either by mass reconstruction or by identifying overlapping showers as described in Sect. 2. A decay candidate was assigned to the $2\pi^0$ decay if there was one charged particle and either 2 photons not forming a π^0, or 3 photons forming one or two π^0's, or 4 photons with two pairs forming π^0's. All other decay candidates with $\geqq3$ photons were attributed to the $\geqq3\pi^0$ decay. These assignments result in 333 "$2\pi^0$-candidates" and 72 "$\geqq3\pi^0$-candidates". In each of these samples substantial background from the other multi-π^0 τ decay channels (feed-up and feed-down) is expected: The signal to background ratios are 1.5:1.0 and 1.1:1.0, respectively. Branching ratios are determined using a transition matrix and a likelihood function in analogy to (1) and (3). The results with their statistical and systematic errors are also shown in Table 5. To obtain the branching fraction for the decay $\tau\to\pi2\pi^0\nu$ a small (0.2%) contribution from $\tau\to K^*\nu$ was subtracted. Figure 6a shows the invariant mass of the hadronic system from the decay $\tau\to\pi2\pi^0\nu$ and the expectation based on an A_1 resonant hadronic state with mass and width typical for determinations from τ decay [7]. The agreement with the Monte Carlo model [21] which was also used for the three charged pion state (Fig. 6b) is satisfactory.

A method similar to the one described above was used to estimate the systematic errors due to uncertainties on the selection, the trigger and scan efficiencies, the photon detection and π^0 reconstruction. To estimate the systematic errors we determined the branching ratios from different types of subsamples (taking, e.g., only the two-photon final states as "$2\pi^0$-candidates"). In addition, the influence of the poorly known invariant mass distribution of the $\pi3\pi^0$ final state on the acceptance calculations was checked by computing the branching ratios assuming only low (<0.9 GeV/c^2) or only high (>1.3 GeV/c^2) invariant masses, respectively. No significant influence was found. The sum of the branching ratios for the two multi-π^0 decay modes is in good agreement with the branching ratio of class 5. Since the two

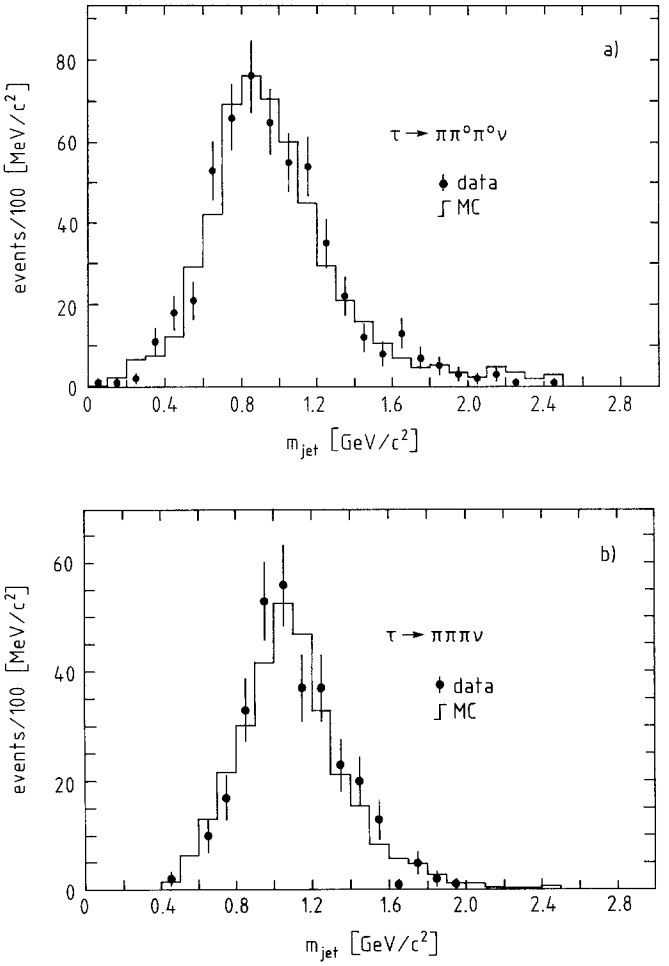

Fig. 6a, b. Invariant mass distributions of **a** one charged particle and all observed photons for the final state classified as $\tau\to\pi2\pi^0\nu$, **b** three charged particles without photons classified as $\tau\to3\pi\nu$. The data points and the expectations from the Monte Carlo (histograms), based on A_1 dominance for the 3 pion system (see text), are shown. Note that in case a the peak is shifted towards lower masses due to unobserved photons lost in regions of reduced acceptance

were obtained by very different analysis methods this agreement is a further check on the correctness of the efficiency calculations based on our Monte Carlo models.

4.3 *Discussion*

All the exclusive branching ratios determined in this analysis are compared in Table 5 with the existing world averages and theoretical expectations based on the standard model [10] and measurements of the τ lifetime (see [7] for a recent review). In almost all cases our results are the most precise determinations by a single experiment.

In general our results are in good agreement with the existing world averages. The branching ratios $\tau^-\to\pi^-\pi^+\pi^-\nu_\tau$ and $\tau^-\to\pi^-\pi^0\pi^0\nu_\tau$ measured in this experiment are larger than previous values. Whereas in our experiment the sum of the multi-π^0 decay modes

of $(13.4 \pm 2.0)\%$ saturates within errors the measured branching ratio of class 5 ($\tau \to$ hadron $+ > 2\gamma$) the sum of $(10.5 \pm 2.8)\%$ of the existing world averages for the same exclusive decay modes does not nearly saturate the semi-inclusive branching ratio for $\tau \to$ hadron $+ \geqq 2$ hadron^0 ν of $(16.3 \pm 1.3)\%$ given in [20]. A similar situation can be noticed for the sum of all branching ratios. Whereas the sum of the existing branching ratio measurements fails to saturate the total τ decay rate by about 2 standard deviations, the same sum measured in our experiment adds up to $(99.8 \pm 2.6 \pm 1.2)\%$ and thus leaves little room for yet undetected or unconventional decay modes. Likewise our previously published inclusive one-prong branching ratio $BR_1 = (84.9 \pm 0.4 \pm 0.3)\%$ is in agreement with the sum of exclusive one prong branching ratios measured in this experiment, namely $BR_1 = (85.0 \pm 2.4 \pm 1.2)\%$.

The agreement between our data and the theoretical expectations is good. It should be noted, however, that the predictions for $BR(\tau \to 3\pi\nu)$ are quite uncertain. The values assumed here come from a particular model based on a pure A_1 resonance [21] and have been chosen to saturate the theoretical branching ratios. Our measurements support this model. In particular, the ratio of $BR(\tau \to \pi 2\pi^0 \nu)/BR(\tau \to 3\pi\nu)$ is predicted to be equal to unity, based on the assumption of a pure A_1 resonance. We find for this ratio the value 1.15 ± 0.24. It should be noted also that isopin symmetry requires this ratio to be less or equal to one. A possible small contribution of the decay $\tau \to \pi\eta\pi^0\nu$ (the branching fraction of which is below 0.7% [20]) to the decay $\tau \to \pi 2\pi^0 \nu$ is still under investigation.

Our measurements can be used to test several predictions of the standard model. As can be seen from Table 5, the branching ratio $\tau \to e\nu\nu$ agrees well with the expectation based on the lifetime measurements (note that another recent measurement of the electronic branching ratio [22] is somewhat lower than the expectation). Universality also predicts the ratio of $BR(\tau \to \mu\nu\nu)/BR(\tau \to e\nu\nu)$ to be 0.973 [4, 10], in very good agreement with our measured value of 0.962 ± 0.067. Based on the CVC hypothesis and the measured cross sections $R(e^+e^- \to 2\pi^+ 2\pi^-)$ and $R(e^+e^- \to \pi^+\pi^- 2\pi^0)$ [4, 10], the ratio $BR(\tau \to \pi 3\pi^0 \nu)/BR(\tau \to 3\pi\pi^0\nu)$ is predicted to be 0.21. We find for this ratio the value 0.57 ± 0.26, in fair agreement with the expectation. However, it should be noted that our value for $BR(\tau \to \pi 3\pi^0 \nu)$ may contain contributions from final states with more than $3\pi^0$'s and, possibly, also from the decay channels $\tau \to \pi\eta \geqq 1\pi^0\nu$.

5 Conclusions

Using data at 35 GeV centre of mass energy corresponding to an integrated luminosity of $87\,pb^{-1}$ collected with the CELLO detector at PETRA, we have measured all the major exclusive branching ratios of the τ lepton simultaneously.

In almost every case our results are the most precise determinations by a single experiment, mostly agreeing well with the world average values. For the decay modes $\tau^- \to \pi^-\pi^+\pi^-\nu_\tau$ and $\tau^- \to \pi^-\pi^0\pi^0\nu_\tau$, however, we observe branching ratios larger than the present world averages. Whereas the sum of the previously existing branching ratio measurements (averaged from many different experiments) fails to saturate the total τ decay rate, our results add up to $(99.8 \pm 2.6 \pm 1.2)\%$ and thus leave little room for undetected decay modes, in particular those of an unconventional kind. The sum of all the exclusive one-prong branching ratios is also in very good agreement with the corresponding inclusive branching ratio recently published by CELLO [12].

All the measured exclusive branching ratios given here are in agreement with the expectations from the standard model.

Acknowledgements. We gratefully acknowledge the outstanding efforts of the PETRA machine group which made these measurements possible. We are indebted to the DESY computer centre for their excellent support during the experiment. We acknowledge the invaluable effort of the many engineers and technicians from the collaborating institutions in the construction and maintenance of the apparatus. The visiting groups wish to thank the DESY Directorate for the support and kind hospitality extended to them.

This work was partially supported by the Bundesministerium für Forschung und Technologie (Germany), by the Commissariat à l'Energie Atomique and the Institut National de Physique Nucléaire et de Physique des Particules (France), by the Istituto Nazionale di Fisica Nucleare (Italy), by the Science and Engineering Research Council (UK), and by the Ministry of Science and Development (Israel).

References

1. M. Perl et al.: Phys. Rev. Lett. 35 (1975) 1489
2. S.L. Glashow: Nucl. Phys. 22 (1961) 579; A. Salam: Elementary particle theory. N. Swartholm (ed.) p. 367. Stockholm: Almquist and Wiksell 1968; S. Weinberg: Phys. Rev. Lett. 19 (1967) 1264; Phys. Rev. Lett. 27 (1971) 1688
3. C. Kiesling: Test of the standard theory of electroweak interactions, Spriger Tracts in Modern Physics, vol. 112. Berlin, Heidelberg, New York: Springer 1988
4. Y.S. Tsai: Phys. Rev. D 4 (1971) 2821
5. H.B. Thacker, J.J. Sakurai: Phys. Lett. 36 B (1971) 103
6. F.J. Gilman, D.H. Miller: Phys. Rev. D 17 (1978) 1846
7. C. Kiesling, τ Physics, in: High energy electron positron physics, A. Ali, P. Söding (eds), p. 716. Singapore: World Scientific 1988
8. K.G. Hayes, M.L. Perl: Phys. Rev. D 38 (1988) 3351
9. D. Wegener: Proc. of the XXIVth International Conference on High Energy Physics, Munich, 1988, p. 877
10. F.J. Gilman, S.H. Rhie: Phys. Rev. D 31 (1985) 1066
11. F.J. Gilman: Phys. Rev. D 35 (1987) 3541
12. H.J. Behrend et al.: Phys. Lett. 222 B (1989) 163
13. H.J. Behrend et al.: Phys. Lett. 114 B (1982) 282
14. H.J. Behrend: Comp. Phys. Commun. 22 (1981) 365
15. H.J. Behrend et al.: Phys. Scr. 23 (1981) 610
16. EGS, R.L. Ford, W.R. Nelson; SLAC report 210 (1978)
17. HETC code, RSIC Computer Code Collection, Oak Ridge National Laboraty, CCC-178
18. W. Wiedenmann: Messung elektroschwacher Effekte und topologischer Verzweigungsverhältnisse in der Reaktion $e^+e^- \to \tau^+\tau^-$ am Speichering PETRA, MPI-PAE/Exp. El. 195 (1988)
19. S. Scholz, MPI-Report, in preparation
20. Particle Data Group: Phys. Lett. 204 B (1988) 1
21. T.N. Pham, C. Roiesnel, T.N. Truong: Phys. Lett. 78 B (1978) 623
22. S. Abachi et al.: Phys. Lett. B 226 (1989) 405